

Line selection in off-resonantly pumped multilevel systems

M. A. Dupertuis* and M. R. Siegrist

Centre de Recherches en Physique des Plasmas, Ecole Polytechnique Fédérale de Lausanne, 21, Avenue des Bains, CH-1007 Lausanne, Switzerland

R. R. E. Salomaa

Department of Technical Physics, Helsinki University of Technology, SF-02150 Espoo 15, Finland

(Received 29 December 1986)

In weakly, off-resonantly pumped multilevel systems gain is usually observed at the transition frequencies (line-center lines) and at the pump-offset-dependent frequencies (Raman lines). Modes developing at these frequencies are subject to strong mutual competition due to several coupling mechanisms. A general six-level system is investigated in this paper. Line competition effects are studied in particular in the simplified basic four-level cases comprising parallel, cascade, and V - Λ subsystems. We predict the type of transitions which survive and ultimately remain active. A comparison with experimental results using far-infrared lasers is made.

I. INTRODUCTION

In off-resonantly pumped systems it is possible to clearly distinguish Raman-type emission from line-center emission. The two processes are also sometimes referred to as parametric or laser-like processes, respectively. Since both emission types are generally able to grow, it is of great importance to be able to predict which one dominates.

A definition of such line-competition problems, and the conditions under which these occur, will be formulated in this paper. The interaction mechanisms between lines and the possible means to influence their mutual competition will be discussed. We shall ignore all resonant-cavity effects. The system is either allowed to choose its own oscillation frequencies or else these are simply imposed as external-boundary conditions.

The main peculiarities of the systems pumped by off-resonant coherent light are certainly due to the coherence of the pump and coupled Doppler effects. Both arise from the fact that the active medium is at least a three-level system interacting with two classical fields. In the homogeneously broadened regime, when the spectral mode density is high enough [cf. Fig. 1(a)], the coarsest level of oscillation competition would occur in line selection between line-center and stimulated Raman emission. On a finer scale several competing cavity eigenmodes can appear within the gain bands of the two above-mentioned lines (especially when inhomogeneity is added).

The oscillation competition situation described above arises in most pulsed optically pumped far-infrared lasers.¹⁻⁵ Often it is of particular interest to obtain single-mode Raman emission since it is tunable by pump tuning. Indeed, tunable far emission from 100 to 1200 μm has been obtained.⁶ This has enabled, for example, the development of notch filters which are important to suppress parasitic stray light in collective Thomson scattering experiments.⁷ In several applications (e.g., plasma diagnostics, high-resolution spectroscopy) it is desirable to have single-mode operation in addition to tunability. Another stimulus for research in this field is offered

by the challenge of efficiency enhancement⁶ which, in principle, may also be posed as a line-competition problem.

The present investigation is also of relevance for the new coherently pumped systems in the mid-ir region^{8,9} and for visible and uv dimer lasers.¹⁰ Recent experiments on four-wave mixing¹¹ have demonstrated the importance of line competition in these devices.

The paper is divided as follows: Sec. II defines the line-competition problem considered, Sec. III briefly summarizes the theory, Sec. IV presents the analysis of the basic three-level case, Sec. V treats the more complicated four-level configurations, and Sec. VI reviews some experimental results which are compared with our theory. Section VII finally gives a discussion and conclusions. The Appendices contain some lengthy formulas for the benefit of particularly interested readers.

II. LINE COMPETITION

The novelty of the present study is the consideration of line competition, which occurs between different sets of modes in an off-resonantly pumped laser. To illustrate our concept of line competition let us consider the gain spectrum of a simple three-level system. In the homogeneously broadened regime two conditions are required to have two distinct gain peaks as in Fig. 1, one at the Raman frequency, and the other one at the line center:

(i) To create the Raman gain the system must be pumped off-resonantly.

(ii) The pump should not be so intense as to induce excessive ac-Stark shifts. (If this were the case, the peaks would tend to occupy symmetric positions around line center and their nature would become mixed rendering the problem more complicated.)

For convenience we also assume that the resonator does not favor any particular oscillation type. We concentrate on the study of the combined effects due to the modes under the Raman line onto the line-center modes or vice versa. The interaction between modes within the two reso-

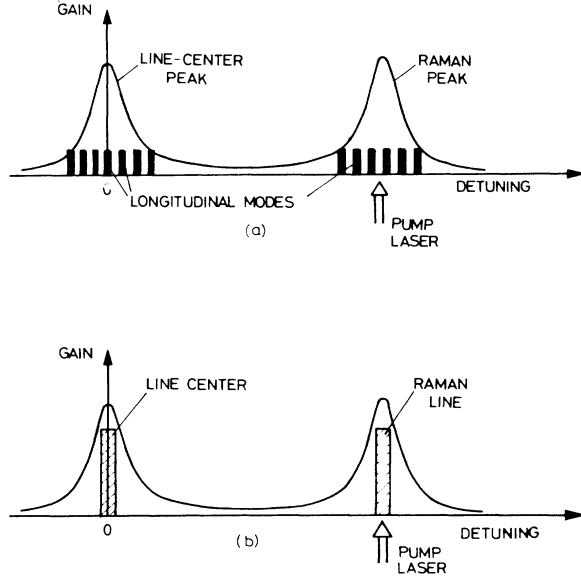


FIG. 1. (a) Mode and line competition under the gain curve of an off-resonantly pumped laser. (b) Model for line competition adopted in this work.

nance lines will be neglected. Hence the competition situation is described by the effective two-mode model of Fig. 1(b).

Within these approximations we have been able to explain the dominance of Raman emission in fir lasers¹² and also found some exceptions to this rule.¹³ Here we will present a more detailed account of these problems, estimate the influence of several parameter dependencies, relax some of our assumptions, and investigate in a more systematic way the basic level configurations. We shall generally ignore space-dependent effects: we treat only unidimensional propagation in an amplifier because the evolution of the field in a cavity obeys similar equations when the validity conditions of a mean-field model are satisfied.¹⁴ Our results hold for cw lasers and pulsed lasers with a pulse length much longer than the medium response time. We shall show that this approach yields interesting general information despite its restrictive assumptions which do not account for transient effects, excessive ac-Stark shifts, inhomogeneous broadening of the signal transitions, and transverse effects, for example.

III. THEORY MODEL

The classical field is composed of the pump mode and the discrete set of signal modes,

$$\mathcal{E}_{ij}(z,t) = \frac{1}{2} \sum_n E_{ij,n} \exp[i(K_{ij,n}z - \Omega_{ij,n}t)] + c.c., \quad (1)$$

where $\mathcal{E}_{ij}(z,t)$ is the amplitude of the electric field near resonant with the transition $i \leftrightarrow j$. The active medium is described in terms of a six-level model (shown in Fig. 2) which corresponds to a configuration often encountered in experiments.^{9,15} Although we give the basic equations

governing such a complex system, we will not study it with all transitions active simultaneously. However, a range of interesting subcases— Λ , V transitions, cascades and parallel configurations—will be treated in detail which provide considerable insight into the mechanisms governing the full system.

The polarization induced by the fields is calculated with the standard density matrix formalism¹⁶ which will only briefly be outlined below. The density matrix $\bar{\rho}$ obeys the equation of motion,

$$i\hbar(\partial_t + v\partial_z)\bar{\rho} = [H, \bar{\rho}] + i\hbar\partial_t\bar{\rho}|_{\text{relax}}, \quad (2)$$

where $\partial_t\bar{\rho}|_{\text{relax}}$ includes incoherent pumping and relaxation of the levels. The Hamiltonian contains the unperturbed part H_0 and the dipole-interaction term $\mu \sum_{ij} \mathcal{E}_{ij}(z,t)$. With the rotating-wave approximation we are allowed to assume that the amplitudes

$$\rho_{ij} = \bar{\rho}_{ij} \exp[-i(K_{ij,0}z - \Omega_{ij,0}t)] \quad (i \neq j), \quad (3)$$

$$\rho_{ii} = \bar{\rho}_{ii}, \quad (4)$$

vary slowly compared to the combination frequencies $\Omega_{ij,n} + \Omega_{kl,m}$. For the central frequencies $\Omega_{ij,0}$ and corresponding wave numbers $K_{ij,0}$ we can pick one of the pairs appearing in (1).

We will now outline the method of solution for the special case where the pump field is single mode and the signal fields are multimode. A more general case has been considered in Ref. 17. Inserting (1) and (3) into (2) we find the equations of motion for the 21 matrix elements of interest (see Appendix A). In these equations, relaxation terms of the form $\Gamma_i(n_i^0 - \rho_{ii})$ and $\gamma_{ij}\rho_{ij}$ have been added, and the detunings Δ_{ij} are equal to $\omega_{ij} - \Omega_{ij} + K_{ij}v$ where ω_{ij} is the frequency the molecular transition $i \leftrightarrow j$. The Rabi frequencies corresponding to the fields \mathcal{E}_{ij} coupling the levels $|i\rangle$ and $|j\rangle$ of Fig. 2 have been denoted by

$$\alpha = \frac{\mu_{12}\mathcal{E}_{12}(z,t)}{2\hbar} \exp[-i(K_{12}z - \Omega_{12}t)], \quad (5)$$

$$\mu = \frac{\mu_{01}\mathcal{E}_{01}(z,t)}{2\hbar} \exp[-i(K_{01}z - \Omega_{01}t)], \quad (6)$$

$$\beta = \frac{\mu_{23}\mathcal{E}_{23}(z,t)}{2\hbar} \exp[-i(K_{23}z - \Omega_{23}t)], \quad (7)$$

$$\epsilon = \frac{\mu_{34}\mathcal{E}_{34}(z,t)}{2\hbar} \exp[-i(K_{34}z - \Omega_{34}t)], \quad (8)$$

$$\zeta = \frac{\mu_{25}\mathcal{E}_{25}(z,t)}{2\hbar} \exp[-i(K_{25}z - \Omega_{25}t)]. \quad (9)$$

The Doppler shifts will always be neglected for the signal transitions; only in one example the effect of the pump Doppler shifts $K_{12}v$ will be included. Similarly the spatial dependence of (5)–(9) will be ignored since we confine the study to corunning waves.

Each one of the signal fields of (6)–(9) can be developed in its mode components [recall the rotating-wave approximation when reducing (5)–(9)]. If the modes are equally spaced in frequency, we get

$$\beta = \sum_{n=0}^{N_\beta} \beta_n \exp(-in\delta t), \quad (10)$$

$$\epsilon = \sum_{n=0}^{N_\epsilon} \epsilon_n \exp(-in\delta t), \quad (11)$$

and so on. This is, for instance, applicable to the situation of line competition where the line spacing δ is dictated by the pump detuning Δ_{21} [cf. Fig. 1(b)].

Assuming that β_n, ϵ_n , etc. do not vary appreciably within $\Gamma_i^{-1}, \gamma_{ij}^{-1}$ we obtain a stationary solution of (2) as a Fourier series,

$$\rho_{ij}(t) = \sum_{m=-\infty}^{+\infty} \rho_{ij}(m) \exp(-im\delta t). \quad (12)$$

The substitution of (12) into (2) leads to recursion relations between the coefficients $\rho_{ij}(m)$. We will not present these here because of their length. Only for the simple case of a three-level system, the details are provided in Appendix B.

The polarization of the medium is given by $\text{Tr}(-\mu\bar{\rho})$. With the aid of Eqs. (3) and (12) we obtain for the polarization

$$\mathcal{P}_{ij}(z, t) = \frac{1}{2} \sum_n P_{ij,n} \exp[i(K_{ij,n}z - \Omega_{ij,n}t)] + \text{c.c.} \quad (13)$$

with

$$P_{ij,n} = -2\mu_{ij}\rho_{ij}(n). \quad (14)$$

Inserting (13) into the Maxwell equations in which we make the slowly varying envelope approximation, and integrating over the beat period δ^{-1} we find for the signal amplitudes

$$\frac{d}{dz} |E_{ij,n}| = \frac{2\hbar G_{ij}}{\mu_{ij}} \text{Im} \left[\frac{\rho_{ij}(n)}{E_{ij,n}} \right] |E_{ij,n}| \quad (15)$$

and for the signal phases

$$\frac{d}{dz} \Phi_{ij,n} = \frac{2\hbar G_{ij}}{\mu_{ij}} \text{Re} \left[\frac{\rho_{ij}(n)}{E_{ij,n}} \right], \quad (16)$$

where the gain factors are defined as

$$G_{ij} = \frac{\mu_{ij}^2 N \Omega_{ij,0}}{2\hbar \epsilon_0 c} \quad (17)$$

and N is the density of the active atoms.

It should be noted that Eq. (13) contains beat notes which act as drivers for new signal modes separated from the original one by multiples of δ . When solving for $\rho_{ij}(n)$ all the modes should be taken into account self-consistently. In the present line-competition problem it is, however, possible to truncate the infinite system of Fourier coefficients (12). This allows us to include self-consistently a finite number of modes in the analysis. Moreover, it is often possible to discard from the outset the modes which will be asymptotically extinguished. However, this cannot always be guessed correctly *a priori* as will be demonstrated below.

IV. THREE-LEVEL SYSTEM

The general configuration of Fig. 2 simplifies to a three-level model when only one of the fir transitions shows appreciable gain. In the following we shall concentrate on the Λ configuration comprising the levels 1, 2 and 3. The V configuration 0,1,2 is completely analogous. The superposition of these three-level cases provides some insight into the full system. The validity of the simple superposition will be checked later on in this paper when the interference effects between Λ and V transitions will be studied.

The free parameters of the model include the pump intensity $|\alpha|^2$ and its detuning Δ , and the intensities ($|\beta_0|^2, |\beta_1|^2$) and detunings of the two fir modes assumed. Of special interest is the case where one of the fir lines is intense and the other one is a weak tunable probe. Small-signal-gain considerations suggest that the intense mode appears either in the vicinity of the line center or the Raman resonance where initially the highest gains are observed. The pump detuning is assumed such that $|\alpha|, |\beta| \ll |\Delta|$ which implies that the fir emission lines still have a clear Raman or line-center character. For large values of α or $\beta_0(\beta_1)$ the fir gain spectrum rather reflects ac-Stark effects. The gain resonances are then due to heavily dressed states for which the terminology Raman or line-center emission is meaningless [a more detailed investigation of probe spectra in these cases is given in Ref. (18)].

We have recently proved¹² that intense-enough Raman oscillation is able to suppress line-center gain through nonlinear interactions between the two lines in the medium: strong line-center absorption appears because of the combined action of population effects, population pulsations, and off-diagonal coherence contributions. The reverse case is not observed, i.e., intense line-center oscillation only splits the Raman gain, but does not invert it (for details see Figs. 2 and 3 of Ref. 12). So the main conclusion is that only Raman emission survives asymptotically in the three-level system. In the following we shall discuss more details of the competition between the line center and the Raman line and relax some approximations made in Ref. 12.

The basic formulas required for calculating the evolution of fir modes are given in Appendix B. Reasonably simple analytical expressions are obtained when we as-

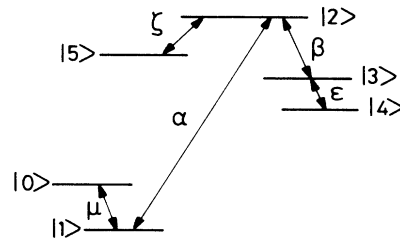


FIG. 2. General six-level configuration considered in this work. The transition $|1\rangle \rightarrow |2\rangle$ is pumped.

sume a weak probe and detuned pump. The probe gain near the line center is obtainable from

$$\rho_{23}(1) = -i \frac{|\alpha|^2}{\Delta^2} \frac{\beta_1}{\gamma_{23}} n_1^0 \left[1 - \frac{2\gamma_{21}}{\Gamma_2} + 2 \frac{|\beta_0|^2}{\Gamma_3 \gamma_{31}} + \frac{|\beta_0|^2}{\gamma_{31} \gamma_{21}} \right] \quad (18)$$

and near the intense Raman oscillation from

$$\rho_{23}(0) = i \frac{|\alpha|^2}{\Delta^2} \frac{\beta_0}{\gamma_{31}} n_1^0. \quad (19)$$

[Notice that in (7) we have assumed $\omega_{21} - \omega_{23} = \Omega_{21} - \Omega_{23}$ which implies that in (10) the mode $n=0$ corresponds to the Raman resonance and the mode $n=1$ to the line center]. If the strong line is at resonance, the probe gain near the Raman peak is given by

$$\rho_{23}(0) = i \frac{|\alpha|^2}{\Delta^2} \frac{\beta_0}{\gamma_{31}} n_1^0 \left[\frac{1}{1 + |\beta_1|^2 / \gamma_{31} \gamma_{21}} \right]. \quad (20)$$

The results (18)–(20) are valid to order Δ^{-2} . The novel feature as compared to Ref. 12 is the possibility of considering unequal relaxation rates. According to (18) the threshold for suppression of line-center oscillation is

$$\beta_{0,\text{th}}^2 = \gamma_{31} \gamma_{21} \left[\frac{\frac{2\gamma_{21}}{\Gamma_2} - 1}{\frac{2\gamma_{31}}{\Gamma_3} + 1} \right], \quad (21)$$

which shows that $\beta_{0,\text{th}}^2$ increases with the transverse relaxation rates γ_{31} and γ_{21} . As the pump incoherence can be roughly described by including an additional contribution to γ_{21} and γ_{31} (see, e.g., Refs. 19 and 20), the expected result follows that the importance of Raman emission decreases also when pump incoherence grows (note that this applies to phase fluctuations only). On the other hand, when the final level lifetime is long ($\Gamma_3 \rightarrow 0$) the threshold (21) is very low; the same happens in the limit $\Gamma_1 \rightarrow 0$ if simultaneously $\gamma_{21} \rightarrow \frac{1}{2}\Gamma_2$ (no phase-changing collisions). If the intermediate level 2 is long lived ($\Gamma_2 \rightarrow 0$), the threshold becomes large and the line-center oscillation is not suppressed.

Under some circumstances Doppler effects are not negligible. Doppler broadening is easily included numerically. In the special case where $Ku \ll \Delta$ and all relaxation rates are equal, a particularly simple analytical expression can be obtained,

$$\rho_{23}(1) = i n_1^0 \frac{\beta_1}{\gamma} \frac{|\alpha|^2}{\Delta^2} \left[1 + \frac{|\beta_0|^2}{\gamma^2} \left\{ \left[\frac{\gamma}{K_{21}u} \right]^2 Z' \left[i \frac{\gamma}{K_{21}u} \right] + 2 \operatorname{Re} \left[i \frac{\gamma}{K_{21}u} Z \left[i \frac{\gamma}{K_{21}u} \right] \right] \right\} \right]. \quad (22)$$

Here Z is the “plasma-dispersion function”²¹ and Z' its derivative. A comparison of (22) to numerical results is given in Fig. 3. The basic effect of Doppler broadening is an increase of the threshold for the inversion of the line-center gain. The physical interpretation is that only one

velocity group sees a Raman resonant pump. It should also be noted that only the Raman peak is Doppler broadened (see Fig. 3), as expected.

Another effect which may alter the simplified line-competition situation treated in Ref. 12 is a nonzero equilibrium population difference between the fir levels. If

$$|n_2^0 - n_3^0|, \frac{\gamma^2}{\Delta^2} |n_2^0 - n_1^0| \gg \frac{\gamma^2}{\Delta^2} |n_2^0 - n_3^0| \quad (23)$$

it is possible to consider also in a simple way the absorption on line center and the dispersion to order γ/Δ . However, already a modest pump intensity

$$\alpha^2 > \Delta^2 \frac{|n_2^0 - n_3^0|}{n_1^0} \quad (24)$$

is able to overcome the linear absorption. Even when Eq. (24) is satisfied intense Raman oscillation is able to suppress the line-center gain. The inequality (23) is usually well satisfied in fir lasers. If this is not the case one has to include many additional terms which all tend to favor line-center oscillation.

Finally, we relax the assumption $\beta, \alpha \ll |\Delta|$ and show some curves illustrating the power of the numerical machinery used for solving the full Eqs. (B2)–(B6) of Appendix B (for more details see Ref. 17). Figure 4 gives an example of a strong probe. The line-center gain disappears even when β_1 approaches saturation which suggests

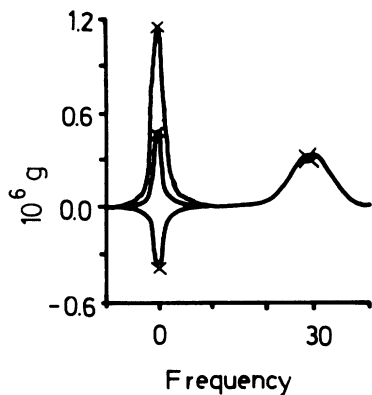


FIG. 3. Influence of Doppler broadening on the linear gain. The quantity g shown is $(1/\gamma)\operatorname{Im}\rho_{23}(1)$. $\Delta_{21} = \Delta_{23} = 30\gamma$, $\alpha = 0.1\gamma$, $\beta_0 = 0.1, 1, 1.5\gamma$ in order of decreasing peak value. $\beta_1 = 0.1\gamma$, $k_{21}u = 5\gamma$, $n_2^0 - n_1^0 = 1$, $n_2^0 - n_3^0 = 0$. The analytical results [Eq. (22)] are represented by crosses.

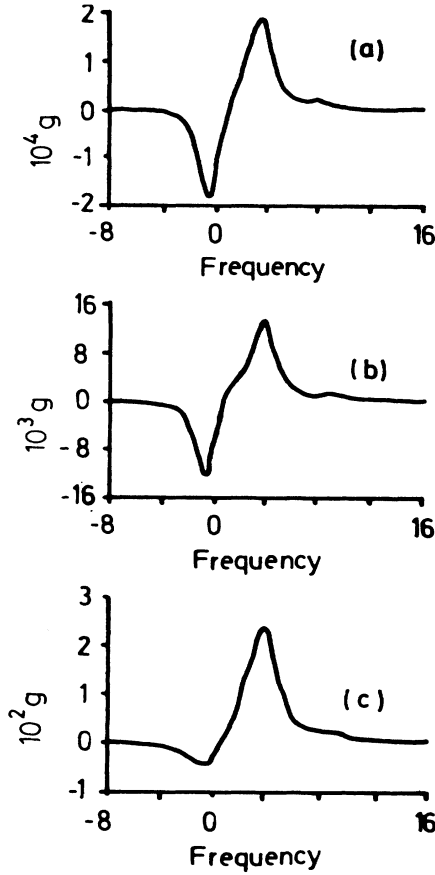


FIG. 4. Strong-probe numerical results. (a) $\Delta_{21}=\Delta_{23}=4\gamma$, $\alpha=0.1\gamma$, $\beta_0=\gamma$, $\beta_1=0.5\gamma$, $k_{21}u=0$, $n_2^0-n_1^0=-1$, $n_2^0-n_3^0=0$. (b) Same as (a) with $\alpha=\gamma$. (c) Same as (a) with $\alpha=\gamma$, $\beta_1=\gamma$.

that the suppression mechanism is also effective during the initial transient period when both modes grow at the same rate (see Ref. 12 for competition dynamics).

An interesting phenomenon is observed when the pump intensity is increased. In Fig. 5 we show a strong-pump case. The two gain peaks are now due to the large ac-Stark effect and no line suppression occurs. As already pointed out these kind of resonances (representing heavily dressed states) are not treated here.

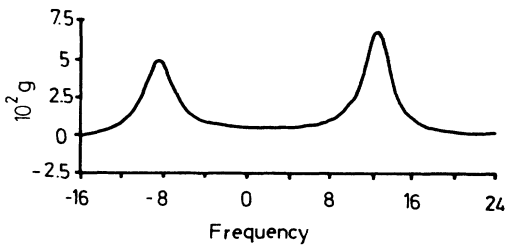


FIG. 5. Numerical results for a strong pump and a strong probe. $\Delta_{21}=\Delta_{23}=4\gamma$, $\alpha=10\gamma$, $\beta_0=3\gamma$, $\beta_1=\gamma$, $k_{21}u=0$, $n_2^0-n_1^0=-1$, $n_3^0=0$.

V. FOUR-LEVEL CASES

Frequently combinations of three-level systems of the type considered above are encountered, especially in fiber lasers.¹⁵ We will now apply the techniques of Sec. III to the basic four-level configurations consisting of the three-level system above and one additional level. As already described in Sec. II our main interest is on competition effects where the transitions considered can be coupled by several field modes. An extensive study on single-mode effects is given Ref. 22. The simplest case is the addition of a cascade transition because we do not need to introduce a new multimode field (to order Δ^{-2}).

A. Cascade

In the case of a cascade transition an additional field denoted by ϵ couples the $3\leftrightarrow 4$ transition (see Fig. 2). In the approximations $n_2^0 \approx n_3^0 \approx n_4^0 \approx 0$ and $|\Delta| \gg \gamma$, the small-signal-gain spectrum of the cascade transition contains only one peak of the order of $1/\Delta^2$ at line center. Resonant single-mode emission on the cascade transition is therefore expected and assumed.

The evolution of the various fields is governed by

$$\frac{d|\alpha|}{dz} = -G_{21}|\alpha| \left[1 + \frac{|\beta_0|^2}{1 + |\beta_1|^2 + |\epsilon|^2} \right], \quad (25)$$

$$\frac{d|\beta_0|}{dz} = G_{23} \frac{|\alpha|^2 |\beta_0|}{1 + |\beta_1|^2 + |\epsilon|^2}, \quad (26)$$

$$\begin{aligned} \frac{d|\beta_1|}{dz} = & G_{23} \frac{|\alpha|^2 |\beta_1|}{(1 + 4|\beta_1|^2 + 4|\epsilon|^2)(1 + |\beta_1|^2 + |\epsilon|^2)} \\ & \times \left[1 - 3|\beta_0|^2 + |\beta_1|^2 + 4|\epsilon|^2 \right. \\ & \left. - \frac{3|\beta_0|^2 |\epsilon|^2}{1 + |\beta_1|^2 + |\epsilon|^2} \right], \quad (27) \end{aligned}$$

$$\begin{aligned} \frac{d|\epsilon|}{dz} = & G_{34} \frac{|\alpha|^2 |\epsilon|}{(1 + 4|\beta_1|^2 + 4|\epsilon|^2)(1 + |\beta_1|^2 + |\epsilon|^2)} \\ & \times \left[2|\beta_0|^2 + 3|\beta_1|^2 - \frac{3|\beta_0|^2 |\beta_1|^2}{1 + |\beta_1|^2 + |\epsilon|^2} \right], \quad (28) \end{aligned}$$

where the dimensionless field amplitudes α, β, ϵ are all in units γ . The stability analysis for single-mode emission on the $2\leftrightarrow 3$ transition is readily performed by analyzing the sign of the line-center gain: according to (27) the threshold for line-center attenuation is

$$|\beta_0|^2 > \frac{1}{3} \frac{(1 + |\beta_1|^2 + 4|\epsilon|^2)(1 + |\beta_1|^2 + |\epsilon|^2)}{1 + |\beta_1|^2 + 2|\epsilon|^2} > \frac{1}{3}. \quad (29)$$

This result indicates that both the line-center oscillation (β_1) and the cascade oscillation (ϵ) increase the threshold. When $|\epsilon|^2 \gg 1$ stable single-mode Raman oscillation is expected for $|\beta_0|^2 > 2|\epsilon|^2/3$. On the other hand, the

same stability analysis can be performed on (28) for ϵ . It shows that cascade oscillation can also be reabsorbed provided that

$$|\beta_0|^2 > \frac{3|\beta_1|^2(1+|\beta_1|^2+|\epsilon|^2)}{|\beta_1|^2-2(1+|\epsilon|^2)} \quad (30)$$

and that $|\beta_1|^2$ exceeds the critical intensity $|\beta_1|^2=2(1+|\epsilon|^2)$. Recall that the Rabi frequencies β, ϵ must be kept below Δ/γ to preserve the conditions of off resonance, but may, in fact, exceed unity by a considerable amount (for more details see Appendix B).

B. $V-\Lambda$ configuration

In some experiments^{9,15} the two three-level transitions of types V and Λ appear simultaneously. Such a case, comprising, for instance, levels 0 to 3 (cf. Fig. 2), is a good example of a more general system with multimode fields in the additional transition. It has been shown¹³ that its nontrivial behavior can still be analyzed rather easily because for a detuned pump the medium response is fortunately analytically tractable. We present in this section a summary of the results of Ref. 13 and give more details about the peculiar behavior of this system.

The refilling oscillation (the flipping rate is denoted by μ , expressed in units of γ) occurs on the $0 \leftrightarrow 1$ transition (Fig. 2) simultaneously with the transition $2 \leftrightarrow 3$ represented by β . We shall again restrict ourselves to the case where the populations at thermal equilibrium satisfy the relations $n_0^0 \approx n_1^0 \approx n^0$ and $n_2^0 \approx n_3^0 \approx 0$. This approximation greatly simplifies the analytical expressions. One can show^{13,23} that the evolution of the fields is governed by

$$\frac{d|\alpha|}{dz} = -G_{12}|\alpha| \left[1 + \frac{1}{\mathcal{D}}[\mathcal{N}(|\mu_0|^2 + |\beta_0|^2) - 4|\mu_0||\beta_0||\mu_1||\beta_1| \cos(\Phi)] \right], \quad (31)$$

$$\frac{d|\mu_0|}{dz} = G_{01} \frac{|\alpha|^2}{\mathcal{D}} [\mathcal{N}|\mu_0| - 2|\mu_1||\beta_1| \cos(\Phi)|\beta_0|], \quad (32)$$

$$\frac{d|\beta_0|}{dz} = G_{23} \frac{|\alpha|^2}{\mathcal{D}} [\mathcal{N}|\beta_0| - 2|\mu_1||\beta_1| \cos(\Phi)|\mu_0|], \quad (33)$$

$$\frac{d|\mu_1|}{dz} = G_{01} \frac{|\alpha|^2|\mu_1|}{1+4|\mu_1|^2} \times \left[1 - \frac{(|\mu_0|^2 - |\beta_0|^2)}{\mathcal{D}} \times [3(1+|\mu_1|^2) + |\beta_1|^2] \right], \quad (34)$$

$$\frac{d|\beta_1|}{dz} = G_{23} \frac{|\alpha|^2|\beta_1|}{1+4|\beta_1|^2} \times \left[1 + \frac{(|\mu_0|^2 - |\beta_0|^2)}{\mathcal{D}} \times [3(1+|\beta_1|^2) + |\mu_1|^2] \right], \quad (35)$$

$$\frac{d\Phi}{dz} = 2 \left[\frac{G_{01}}{|\mu_0|^2} + \frac{G_{23}}{|\beta_0|^2} \right] \times \frac{|\alpha|^2}{\mathcal{D}} |\mu_0||\beta_0||\mu_1||\beta_1| \sin(\Phi). \quad (36)$$

As expected the equations are symmetric with respect to $\{\beta_0, \beta_1\}$, $\{\mu_0, \mu_1\}$. When one of the pairs is neglected, the three-level expressions of Ref. 12 are recovered. Despite the approximation of a detuned pump, the field gain factors still contain considerable saturation and mode coupling.

A novel feature is the high-order dispersion represented by the global phase $\Phi = \phi(\beta_0) - \phi(\beta_1) - \phi(\mu_0) + \phi(\mu_1)$. Its physical origin is the interference between the two “three-photon-resonant paths” $\{\mu_0, \alpha, \beta_1\}$ and $\{\mu_1, \alpha, \beta_0\}$ bringing the system from level 0 to level 3. Another new feature is the appearance of $|\beta_0|^2$ in Eq. (34). It is partly due to population refilling and partly due to a coherence effect.¹³ When $|\mu_0|^2 > |\beta_0|^2$, the dominance of Raman oscillation β_0 typical of the pure three-level case disappears [cf. Eq. (18)]. The competition between the Raman modes μ_0 and β_0 (i.e., the sign of the factor $|\mu_0|^2 - |\beta_0|^2$) determines which line-center mode will survive in the presence of the Raman oscillations.

According to Eq. (36), the phase Φ tends to lock to a value $\Phi_\infty = \pi$ ($\Phi_\infty = 0$ is unstable). Therefore asymptotically $\cos(\Phi)$ turns negative and the two Raman modes assist each other according to Eqs. (32) and (33). The Raman mode having the higher linear gain (G_{01} or G_{23}) will grow faster even when saturation sets in. According to (34) and (35) the ultimately suppressed line-center mode will be μ_1 in the case $|\mu_0|^2 > |\beta_0|^2$ and β_1 in the case $|\mu_0|^2 < |\beta_0|^2$ in the limit $|\mu_0|, |\beta_0| \gg 1$. We may thus conclude that asymptotically the four-level system will oscillate on *both* the Raman and line-center modes at the transition with lower small-signal gain, and only on the Raman mode at the transition with higher gain. Whether this asymptotic solution is realized in an experiment will depend on the length of the amplifier as compared to the two gain lengths involved. It is also worthwhile noticing that this asymptotic solution, chosen by the system, is a compromise between the single-mode Raman-Raman solution expected from the superposition of two three-level systems, and the single-mode line-center-Raman solution expected from energy conservation (without relaxation) between the initial and the final level.

The analysis of Eqs. (32)–(36) reveals that the Raman modes are strongly coupled while the line-center modes are weakly coupled. The Raman–line-center coupling is asymmetric as discussed in Ref. 12, i.e., line-center modes

are strongly coupled to the Raman modes whereas Raman modes are weakly coupled to the line-center modes. The form of the gain equations for the Raman mode suggests that the coupled Raman modes behave as bichromatic modes.^{18,24-26} In Appendix C it is shown that further insight into the behavior of the system may be gained using this picture. We simply recall here that the properties of the bichromatic Raman-Raman modes enable us to show rigorously that the dominant Raman component of the more strongly amplified bichromatic mode (with the largest eigenvalue λ_+) is on the transition where the small signal gain is larger. Estimates of the distance to steplike phase locking have also been obtained.

Finally, some comments are worth making on the limitations of our present study. Firstly, the introduction of cavity losses and external dispersion may considerably alter the results. The latter effect is interesting because a "constant" term is added to the phase equation (36). Unlocked solutions of the system are obtained if the constant term exceeds the coefficient of the sine. In this case the phase Φ rotates and the competition between the Raman modes alternates between mutual enhancement and suppression. The coefficients in (36) depend, however, also on the intensities which complicates the problem. Self-pulsing and chaos are not unlikely to appear when the saturation (to higher orders than Δ^{-2}) of the Raman mode is taken into account.

Another point worth mentioning is that phase noise may be important in the asymptotic stage where one of

the line-center modes has decayed back to noise level. Phase fluctuations can be modeled by a Langevin force acting on the right-hand side of the phase-locking equation. It is possible to show that the Raman-mode phases are adjusted on the invariant line-center mode phases (notice that dispersion vanishes at line center) in order to recall the global phase. Therefore phase noise at the attenuated line-center mode frequency will trigger phase fluctuations on the Raman modes. This "amplified" phase noise is expected to be inversely proportional to the Raman-mode intensity as is the restoring force in the phase equation.

C. Parallel transitions

The last and mathematically most complicated case is the parallel configuration formed by levels 1-3 and 5 in Fig. 2. The additional field coupling the parallel transition $2 \leftrightarrow 5$ is denoted by ζ , again in units of γ . Even stronger phase dependencies than in the previous example are expected because the two-mode transitions share a common level. Stable simultaneous single-mode Raman-Raman operation is intuitively expected, but interference, population transfer, population pulsations, and coherence effects may alter this picture.

Lengthy calculations lead to the following result for the evolution of the modes (within the same approximations as before):

$$\frac{d|\alpha|}{dz} = -G_{21} |\alpha| \left[1 + |\mu_0|^2 + |\beta_0|^2 - \frac{1}{\mathcal{N}} [|\beta_0|^2 |\beta_1|^2 + |\zeta_0|^2 |\zeta_1|^2 + 2 |\beta_0||\beta_1||\zeta_0||\zeta_1| \cos(\Phi)] \right], \quad (37)$$

$$\frac{d|\beta_0|}{dz} = G_{23} \frac{|\alpha|^2}{\mathcal{N}} [|\beta_0| (1 + |\zeta_1|^2) - |\beta_1||\zeta_1| \cos(\Phi) |\zeta_0|], \quad (38)$$

$$\frac{d|\zeta_0|}{dz} = G_{25} \frac{|\alpha|^2}{\mathcal{N}} [|\zeta_0| (1 + |\beta_1|^2) - |\beta_1||\zeta_1| \cos(\Phi) |\beta_0|], \quad (39)$$

$$\begin{aligned} \frac{d|\beta_1|}{dz} = G_{23} \frac{|\alpha|^2}{\mathcal{N}\mathcal{D}} \{ & |\beta_1| [\mathcal{N}^2 - |\beta_0|^2 (3 + 3|\beta_1|^2 + 13|\zeta_1|^2 + 4|\beta_1|^2|\zeta_1|^2 + 4|\zeta_1|^4) \\ & + 2|\zeta_0|^2|\zeta_1|^2 (5 + 2|\beta_1|^2 + 2|\zeta_1|^2)] - |\zeta_1||\zeta_0||\beta_0| \cos(\Phi) E(\beta_1, \zeta_1) \}, \end{aligned} \quad (40)$$

$$\begin{aligned} \frac{d|\zeta_1|}{dz} = G_{25} \frac{|\alpha|^2}{\mathcal{N}\mathcal{D}} \{ & |\zeta_1| [\mathcal{N}^2 - |\zeta_0|^2 (3 + 3|\zeta_1|^2 + 13|\beta_1|^2 + 4|\zeta_1|^2|\beta_1|^2 + 4|\beta_1|^4) \\ & + 2|\beta_0|^2|\beta_1|^2 (5 + 2|\zeta_1|^2 + 2|\beta_1|^2)] - |\beta_1||\beta_0||\zeta_0| \cos(\Phi) E(\zeta_1, \beta_1) \}, \end{aligned} \quad (41)$$

$$\frac{d\Phi}{dz} = 2 \frac{|\alpha|^2}{\mathcal{D}} |\beta_0||\zeta_0||\beta_1||\zeta_1| \sin(\Phi) \left[\frac{G_{23}}{|\beta_0|^2} + \frac{G_{25}}{|\zeta_0|^2} + \left[\frac{G_{23}}{|\beta_1|^2} + \frac{G_{25}}{|\zeta_1|^2} \right] \frac{3 + |\beta_1|^2 + |\zeta_1|^2}{\mathcal{N}} \right], \quad (42)$$

where the function E is defined by the expression

$$E(\beta_1, \zeta_1) = (3 - 7|\beta_1|^2 + 13|\zeta_1|^2 - 4|\beta_1|^4 + 4|\zeta_1|^4). \quad (43)$$

(The global phase Φ stands now for $[\phi(\beta_0) - \phi(\beta_1)$

$-\phi(\zeta_0) + \phi(\zeta_1)]$.) These equations are considerably more complicated than in the previous cases. For instance, there are additional contributions to the line-center gains. In fact, from the evolution equation of the relevant density matrix element,

$$\rho_{23}(1) = i\beta_0 l_{23}(1) D_{23}(1) + i\beta_1 l_{23}(1) D_{23}(0) - ial_{23}(1) \rho_{31}^*(-1) - i\xi_1 l_{23}(1) \rho_{53}(0), \quad (44)$$

we see that a direct coupling with the parallel transition is introduced via the ρ_{53} coherence. Although a deeper analysis of the different contributions to the result above is beyond the present scope, it is still possible to distinguish some features of these equations.

Features similar to the V - Λ configurations include the following:

- The global phase locks to π .
- The two Raman modes enhance each other.
- Strong Raman oscillation tends to suppress line-center operation on the same transition via the processes discovered in Ref. 12.

New features include the following:

- The strongest line-center mode now slightly favors the Raman oscillation on the other transition, e.g., due to the factor $(1 + |\xi_1|^2)$ in (38).
- Simultaneous Raman and line-center oscillation on a signal transition strongly assists line-center oscillation on the other transition, e.g., due to the factor $2|\xi_0|^2|\xi_1|^2(5 + \dots)$ in (40).

●Strong coupling between the line-center modes now exists, as expected. Strong competition or mutual enhancement can occur in (40) and (41), depending on the sign of $\cos(\Phi)$ and the function E .

According to (42), $\cos(\Phi)$ tends to -1 . Therefore its sign will not be discussed any more. The sign of the remaining expression E appearing in (40) and (41) is shown in Fig. 6 as a function of $|\beta_1|^2$ and $|\xi_1|^2$. We can deduce from this figure that, except for a narrow band around $|\beta_1|^2 = |\xi_1|^2$, the strongest line-center mode is enhanced and the weakest one is attenuated due to the terms containing the function E .

Let us now address the important question whether the asymptotic state is a multimode state. In the affirmative

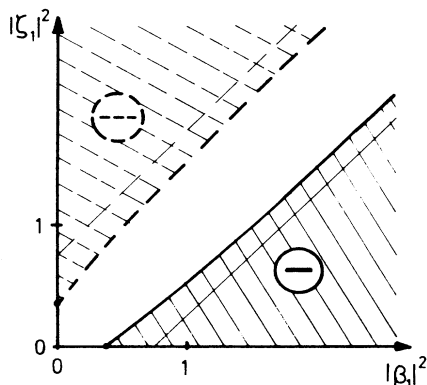


FIG. 6. Sign of the function $E(\beta_1, \xi_1)$ defined by Eq. (43). The dashed part of the figure corresponds to the symmetric expression $E(\xi_1, \beta_1)$ appearing in (41). In the central region where $|\beta_1| \approx |\xi_1|$ the terms containing the function E in Eqs. (40) and (41) contribute to mutual assistance between the line-center modes [if $\cos(\Phi) = -1$]. Outside this region the terms contribute to competition and the weakest line-center mode is favored.

case we would also like to know how many modes are involved. When pump absorption is neglected, Eqs. (38) and (39) reveal that the Raman modes are amplified. A single-mode asymptotic state can, therefore, only be such that $|\xi_0|, |\beta_0| \gg 1$ and $|\xi_1|, |\beta_1| \ll 1$ with $\Phi = \pi$. In this case it is easy to show that

$$\left[\frac{d|\xi_1|}{dz} \frac{d|\beta_1|}{dz} \right] \approx -9|\beta_0||\xi_0|(|\xi_0||\xi_1| - |\beta_0||\beta_1|)^2 < 0. \quad (45)$$

From this we conclude that one of the line-center modes is amplified as well. Let us therefore assume that the asymptotic state is such that three modes oscillate simultaneously. For example, we assume that only the mode β_1 is weak ($|\beta_1| \ll 1$). Equation (40) reveals immediately that this situation is unstable since $d|\beta_1|/dz$ is positive because the function $E(\beta_1, \xi_1)$ is now positive (cf. Fig. 6). The asymptotic state is therefore a multimode state with *all* the modes oscillating simultaneously.

VI. RELATED EXPERIMENTAL RESULTS IN THE FAR INFRARED

In numerous experiments Raman emission in the three-level configuration has been observed.^{5,6,7,27-30} Generally also the cascade emission has been reported as resonant and nontunable.^{28,31,32} On the other hand, apparently contradictory observations have been made on the V - Λ case and much less detailed experimental work has been carried out in the case of parallel transitions. To test if our theory is applicable we will first review some results for the V - Λ case which seem to contradict our theory. We will then show that the asymptotic state predicted in Sec. V has been observed by De Martino, Frey, and Pradère³¹ in the HF molecule.

Woskoboinikow *et al.*²⁸ have demonstrated that the 385- μm line of D_2O is definitely a Raman line and that the "refilling" oscillation at 239 μm is resonant. The measurements and conclusions are quite convincing. It should, however, be noticed that the measurement at 239 μm is close to the noise level and that the spacings in the Fabry-Perot scan are not perfectly regular. Therefore, it is difficult to exclude the possibility of a simultaneous Raman oscillation which should take place according to Sec. VB. Of course, some approximations of our model are perhaps not justified in the experiment (e.g., quasistationarity).

Petuchowski *et al.*²⁹ have established that the 50 and 66- μm lines of D_2O forming a V - Λ configuration are Raman transitions. Their method of measurement was, however, insensitive to a simultaneous line-center oscillation at 50 or 66 μm .

Woskoboinikow *et al.*³² observed that the 257- μm emission in NH_3 is tunable while the coupled emission at 2.14 mm is resonant. In this case, however, the system comprised a Fox-Smith mode selector which influenced the competition.

We now discuss an experiment performed under conditions close to our theoretical hypotheses.³¹ The results reproduced in Fig. 7 display indeed a simultaneous

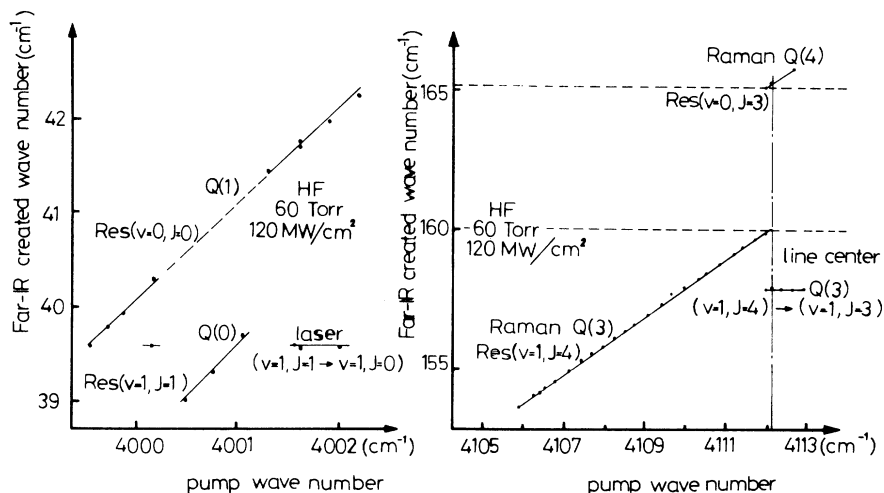


FIG. 7. Details of the experimentally measured tuning curve [reproduced from De Martino, Frey and Pradère (Ref. 31)]. Near the pump wave number of 4112 cm^{-1} simultaneous Raman and line-center oscillation is observed on one signal transition [$Q(3)$], but on the other one [$Q(4)$] only the Raman line oscillates.

Raman–line-center oscillation on the *same* signal transition. A detailed study is necessary to show that the hypotheses of our theory are reasonably well satisfied for these particular conditions. Near the jumps between two $Q(J)$ transitions, two four-level configurations are in competition (Fig. 8). In the four-level configuration related to one $Q(J)$ transition (cf. Fig. 9) the Raman gain is proportional to

$$\begin{aligned} & \left[\frac{\mu_{J,J+1}\mu_{J+1,J}}{\Delta\omega_1} - \frac{\mu_{J,J-1}\mu_{J-1,J}}{\Delta\omega_2} \right]^2 \\ &= \left[\frac{\mu_{J,J+1}\mu_{J+1,J}}{\Delta\omega_1} \right]^2 + \left[\frac{\mu_{J,J-1}\mu_{J-1,J}}{\Delta\omega_2} \right]^2 \\ & \quad - \frac{2\mu_{J,J+1}\mu_{J+1,J}\mu_{J,J-1}\mu_{J-1,J}}{\Delta\omega_1\Delta\omega_2}. \end{aligned} \quad (46)$$

The last term results from an interference between the two paths bringing the molecule from level J , $v=0$ to level J , $v=1$. When the pump is close to resonance in one subsystem the contribution of the other one is negligible because

$$\Delta\omega_1 \gg \Delta\omega_2 \quad (47)$$

or vice versa. Hence in each four-level configuration one of the three-level subsystems is negligible and the result is a four-level V - Λ configuration (see Fig. 8).

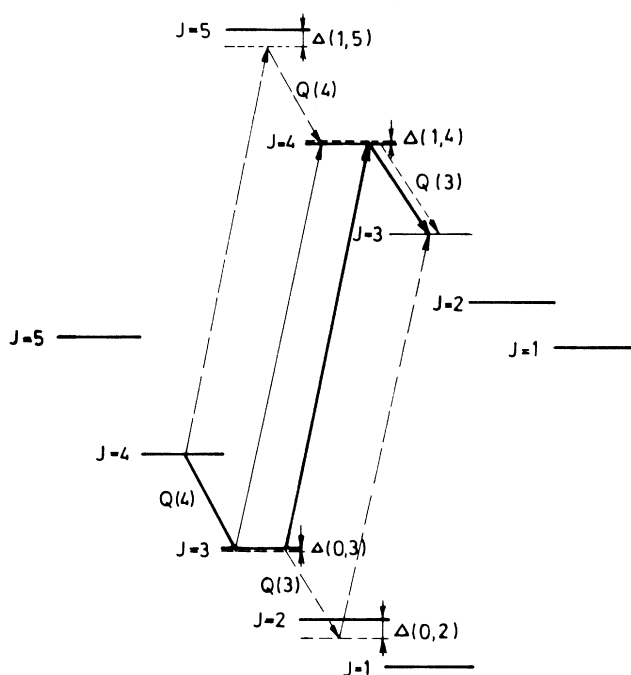


FIG. 8. Relevant level configuration near the jump between two successive $Q(J)$ transitions.

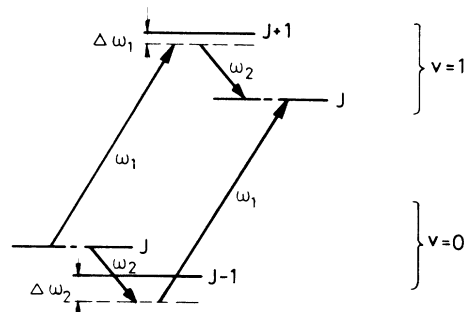


FIG. 9. Level configuration corresponding to one $Q(J)$ pump transition in HF.

In Fig. 7 the structure of the tuning curve near the jump is shown in detail with the identification of the oscillating lines. Near 162.5 cm^{-1} the Raman modes are extinguished because of the rotational absorption band in $\nu=0$, $J=3 \rightarrow J=4$. When the pump is near the resonance $R(3)$,³³ we notice that the system oscillates only in the Raman mode in agreement with Ref. 12. Near this point the detuning changes sign and, according to (46), the interference term hinders the coexistence of the Raman modes beyond the resonance. However, the interference term is very small because condition (47) is verified and should not influence the position of the jump as explained in Ref. 6 in the case of $R(J)$ pump transitions. Indeed one sees on the detailed tuning curve (Fig. 7) that for a pump-laser detuning near 4112 cm^{-1} the asymptotic oscillation state predicted by our theory is observed: Raman line and line center are simultaneous on one signal transition and on the other one only Raman line oscillates.

It is also possible to verify that practically all the conditions of our theory are satisfied because of the following.

- There is no lethargic gain (see, e.g., Refs. 34 and 35); at 60 Torr $\tau_R \sim \frac{1}{6} \text{ nsec} \ll 2.5 \text{ nsec}$ (pulse duration).

- The envelopes are slowly varying: $\Delta_{\text{jump}}^{-1} \sim \frac{1}{60} \text{ nsec} \ll 2.5 \text{ nsec}$.

- There is no dynamic Stark effect which would manifest itself as a curvature in the tuning curve.³⁶

Only the hypothesis $n_0^0 \approx n_1^0$ does not hold very well; this probably contributes to the extinction of the line-center mode on the lower signal transition. If we read off the gain of the fir fields in Fig. 2 of Ref. 31 in the region of the jump at 4112 cm^{-1} we find that simultaneous line-center-Raman operation occurs on the transition with the smallest small-signal gain in agreement with our theory. With a detailed modeling it should be possible to predict the exact shape of the tuning curve since HF is a simple and accurately known molecule.

Several experiments on similar systems are currently under way in a number of laboratories.^{37,38} Some of them could allow a more detailed comparison with our theory.

VII. DISCUSSION AND CONCLUSIONS

The study of line competition in off-resonantly pumped systems carried out in this paper is feasible only as long as the concept of a line is well defined. The requirements for this were postulated in Sec. II.

Because there are close similarities between the case of an oscillator and an amplifier, only the latter case has been considered. In an experimental system the approximation of a quasi-steady-state can sometimes break down during the build-up phase of fir oscillation. However, our assumptions would still hold during the main part of the pulse. Some transient effects, like the one described and explained with simple population arguments by Wiggins *et al.*,³⁰ would require modifications of our theory.

We have first investigated in Sec. IV the influence of additional effects in a basic three-level case to check the generality of the results obtained in Ref. 12. We have shown that pump laser incoherence, various relaxation

rates, and Doppler broadening generally increase (recall the exception $\Gamma_1, \Gamma_3 \rightarrow 0$) the threshold for line-center-oscillation suppression but do not change the main physics discussed in Ref. 12. Numerical examples valid for strong probe fields and nonzero equilibrium population differences ($n_2^0 \neq n_3^0$) on the signal transition, have shown that the validity range of the results is even larger than expected.

In Sec. V, the effects of coupled transitions have been investigated. Among the numerous possible configurations, we have isolated three different four-level configurations which appear as basic elements of the more complicated oscillation schemes frequently encountered in experiments. In order of increasing complexity, we have considered the cascade, the V - Λ , and parallel transitions.

We found that cascade emission is not a major perturbing factor. Its main effect is to increase the stability threshold for single-mode Raman oscillation.

The coupling in the combined Λ and V system was found to be quite strong. The different contributions to the signal gains can be identified analytically, and the importance of nonlinear dispersion has been shown. The system is driven into Raman-Raman oscillation but it also sustains line-center emission on one of the transitions. Further insight in the physical behavior of the system has been enabled by the use of the bichromatic Raman-Raman modes (Appendix C).

The case of parallel transitions resulting from the coupling of two Λ or two V configurations turns out to be the most complicated one, despite its apparent simplicity. A new feature is the strong coupling of the line-center modes. We have been able to show that the asymptotic state of the system is again a multimode state. This non-trivial result demonstrates the importance of all the contributions of the various intertwined effects discovered previously (populations, population pulsations, coherences, interferences).

The general line-selection problem can be summarized in the following way which is more a presentation of intuitive guidelines than of general prescriptions:

- Raman emission is strongly favored on all transitions coupled to the off-resonantly-pumped ones.

- Raman oscillation tends to suppress line-center oscillation on the same transition.

- Raman oscillation may strongly assist line-center oscillation on another transition.

- Cascade oscillation is generally expected to be resonant.

- Interference effects are associated with closed paths within the system of active transitions. As a consequence a phase equation has to be added to the set of evolution equations. In this case transverse effects may become extremely important since Raman and line-center fields can have different directions of propagation because of dispersion (conservation of momentum). The calculation of the local response of the atoms presented here would still apply. Only the field-propagation equation must be modified.

The discovery of several unexpected effects suggests that both analytical calculations and numerical codes are required to solve each special case. Computer codes

designed for algebraic manipulations would be very efficient tools for deriving the laborious analytical expressions.

A variety of different experimental results has been reviewed. Some experiments under conditions close to our theoretical treatment have been found. They agree qualitatively with our results. Many experimental situations remain, however, out of reach of a detailed theoretical line-competition study.

ACKNOWLEDGMENTS

We would like to thank Dr. R. Frey for the kind permission to reproduce Fig. 7.

APPENDIX A

From Eqs. (2), (3), and (5)–(9) we obtain the 21 equations for the density matrix elements. These are given here for the reader's convenience,

$$\dot{\rho}_{00} = \Gamma_0(n_0^0 - \rho_{00}) - 2 \operatorname{Im}(\mu^* \rho_{01}), \quad (\text{A1})$$

$$\dot{\rho}_{11} = \Gamma_1(n_1^0 - \rho_{11}) + 2 \operatorname{Im}(\mu^* \rho_{01} + \alpha^* \rho_{21}), \quad (\text{A2})$$

$$\begin{aligned} \dot{\rho}_{22} = & \Gamma_2(n_2^0 - \rho_{22}) \\ & - 2 \operatorname{Im}(\alpha^* \rho_{21} + \beta^* \rho_{23} + \zeta^* \rho_{25}), \end{aligned} \quad (\text{A3})$$

$$\dot{\rho}_{33} = \Gamma_3(n_3^0 - \rho_{33}) + 2 \operatorname{Im}(\beta^* \rho_{23} - \epsilon^* \rho_{34}), \quad (\text{A4})$$

$$\dot{\rho}_{44} = \Gamma_4(n_4^0 - \rho_{44}) + 2 \operatorname{Im}(\epsilon^* \rho_{34}), \quad (\text{A5})$$

$$\rho_{55} = \Gamma_5(n_5^0 - \rho_{55}) + 2 \operatorname{Im}(\zeta^* \rho_{25}), \quad (\text{A6})$$

$$\dot{\rho}_{01} = -(\gamma_{01} + i\Delta_{01})\rho_{01} + i\mu(\rho_{00} - \rho_{11}) + i\alpha\rho_{20}^*, \quad (\text{A7})$$

$$\begin{aligned} \dot{\rho}_{21} = & -(\gamma_{21} + i\Delta_{21})\rho_{21} + i\alpha(\rho_{22} - \rho_{11}) \\ & - i\beta\rho_{31} - i\zeta\rho_{51} + i\mu\rho_{20}, \end{aligned} \quad (\text{A8})$$

$$\begin{aligned} \dot{\rho}_{23} = & -(\gamma_{23} + i\Delta_{23})\rho_{23} + i\beta(\rho_{22} - \rho_{33}) \\ & - i\alpha\rho_{31}^* - i\zeta\rho_{53} + i\epsilon^*\rho_{24}, \end{aligned} \quad (\text{A9})$$

$$\begin{aligned} \dot{\rho}_{34} = & -(\gamma_{34} + i\Delta_{34})\rho_{34} + i\epsilon(\rho_{33} - \rho_{44}) \\ & - i\beta^*\rho_{24}, \end{aligned} \quad (\text{A10})$$

$$\dot{\rho}_{54} = -(\gamma_{54} + i\Delta_{54})\rho_{54} - i\zeta^*\rho_{24}, \quad (\text{A11})$$

$$\begin{aligned} \dot{\rho}_{20} = & -(\gamma_{20} + i\Delta_{20})\rho_{20} - i\alpha\rho_{01}^* - i\beta\rho_{30} \\ & - i\zeta\rho_{50} + i\mu^*\rho_{21}, \end{aligned} \quad (\text{A12})$$

$$\begin{aligned} \dot{\rho}_{31} = & -(\gamma_{31} + i\Delta_{31})\rho_{31} - i\beta^*\rho_{21} - i\epsilon\rho_{41} \\ & + i\mu\rho_{30} + i\alpha\rho_{23}^*, \end{aligned} \quad (\text{A13})$$

$$\begin{aligned} \dot{\rho}_{24} = & -(\gamma_{24} + i\Delta_{24})\rho_{24} - i\alpha\rho_{41}^* - i\beta\rho_{34} \\ & - i\zeta\rho_{54} + i\epsilon\rho_{23}, \end{aligned} \quad (\text{A14})$$

$$\begin{aligned} \dot{\rho}_{53} = & -(\gamma_{53} + i\Delta_{53})\rho_{53} - i\zeta^*\rho_{23} \\ & - i\beta\rho_{25}^* + i\epsilon^*\rho_{54}, \end{aligned} \quad (\text{A15})$$

$$\begin{aligned} \dot{\rho}_{30} = & -(\gamma_{30} + i\Delta_{30})\rho_{30} - i\beta^*\rho_{20} \\ & - i\epsilon\rho_{40} + i\mu^*\rho_{31}, \end{aligned} \quad (\text{A16})$$

$$\begin{aligned} \dot{\rho}_{41} = & -(\gamma_{41} + i\Delta_{41})\rho_{41} - i\epsilon^*\rho_{31} \\ & + i\mu\rho_{40} + i\alpha\rho_{24}^*, \end{aligned} \quad (\text{A17})$$

$$\begin{aligned} \dot{\rho}_{25} = & -(\gamma_{25} + i\Delta_{25})\rho_{25} + i\zeta(\rho_{22} - \rho_{55}) \\ & - i\alpha\rho_{51}^* - i\beta\rho_{53}^*, \end{aligned} \quad (\text{A18})$$

$$\dot{\rho}_{40} = -(\gamma_{40} + i\Delta_{40})\rho_{40} - i\epsilon^*\rho_{30} - i\mu^*\rho_{41}, \quad (\text{A19})$$

$$\begin{aligned} \dot{\rho}_{51} = & -(\gamma_{51} + i\Delta_{51})\rho_{51} - i\zeta^*\rho_{21} \\ & + i\mu\rho_{50} + i\alpha\rho_{25}^*, \end{aligned} \quad (\text{A20})$$

$$\dot{\rho}_{50} = -(\gamma_{50} + i\Delta_{50})\rho_{50} - i\zeta^*\rho_{20} + i\mu^*\rho_{51}. \quad (\text{A21})$$

Here the dot stands for the convective derivative.

APPENDIX B

We calculate the matrix elements only for the basic three-level case to order Δ^{-2} . The insertion of Eq. (12) as well as

$$\beta = \beta_0 + \beta_1 \exp(-i\delta t) \quad (\text{B1})$$

into the equations of Appendix A (for $\mu = \epsilon = \zeta = 0$) leads to

$$\begin{aligned} D_{21}(p) = & -n_1^0 \delta_{p,0} + i[L_2(p) + L_1(p)] \\ & \times [\alpha^* \rho_{21}(p) - \alpha \rho_{21}^*(-p)] \\ & + iL_2(p)[\beta_0^* \rho_{23}(p) - \beta_0 \rho_{23}^*(-p) \\ & + \beta_1^* \rho_{23}(p+1) - \beta_1 \rho_{23}^*(-p+1)], \end{aligned} \quad (\text{B2})$$

$$\begin{aligned} D_{23}(p) = & iL_2(p)[\alpha^* \rho_{21}(p) - \alpha \rho_{21}^*(-p)] \\ & + i[L_2(p) + L_3(p)] \\ & \times [\beta_0^* \rho_{23}(p) - \beta_0 \rho_{23}^*(-p) \\ & + \beta_1^* \rho_{23}(p+1) - \beta_1 \rho_{23}^*(-p+1)], \end{aligned} \quad (\text{B3})$$

$$\begin{aligned} \rho_{21}(p) = & i\alpha l_{21}(p) D_{21}(p) - i\beta_0 l_{21}(p) \rho_{31}(p) \\ & - i\beta_1 l_{21}(p) \rho_{31}(p-1), \end{aligned} \quad (\text{B4})$$

$$\begin{aligned} \rho_{23}(p) = & i\beta_0 l_{23}(p) D_{23}(p) + i\beta_1 l_{23}(p) D_{23}(p-1) \\ & - i\alpha l_{23}(p) \rho_{31}^*(-p), \end{aligned} \quad (\text{B5})$$

$$\begin{aligned} \rho_{31}(p) = & i\alpha l_{31}(p) \rho_{23}^*(-p) - i\beta_0^* l_{31}(p) \rho_{21}(p) \\ & - i\beta_1^* l_{31}(p) \rho_{21}(p+1), \end{aligned} \quad (\text{B6})$$

where we have used the following definitions:

$$D_{ij}(p) = \rho_{ii}(p) - \rho_{jj}(p), \quad (\text{B7})$$

$$L_j(p) = (\Gamma_j - ip\delta)^{-1}, \quad (\text{B8})$$

$$l_{jk}(p) = [\gamma_{jk} + i(\Delta_{jk} - p\delta)]^{-1}. \quad (\text{B9})$$

As outlined earlier we assume the following:

●The mode with index 0 is at the Raman resonance,

$$\Delta_{23} = \Delta_{21} = \Delta.$$

●The mode with index 1 is at line center

$$\delta = \Delta.$$

●The detuning is large,

$$\Delta \gg \Gamma_j, \gamma_{jk}, \alpha, \beta.$$

The last assumption allows us to expand in $(1/\Delta)$. The Lorentzians are all of first order except $l_{31}(0), l_{21}(1), l_{23}(1)$ which are of zeroth order. From the examination of the infinite linear system (B2)–(B6) it can be inferred that the order of the matrix elements is the following:

●Zeroth order: $D_{21}(0)$,

●First order: $\rho_{21}(0), \rho_{21}(1), \rho_{31}(0)$,

●Second order: $\rho_{23}(0), \rho_{23}(1), D_{23}(0), D_{21}(\pm 1), D_{23}(\pm 1), \rho_{31}(\pm 1)$.

All other elements are of higher order.

The full system (B2)–(B6) can now be truncated to second order which gives the following self-consistent set:

$$D_{21}(0) = -n_1^0 - 2[L_2(0) + L_1(0)]\text{Im}[\alpha^* \rho_{21}(0)] - 2L_2(0)\text{Im}[\beta_0^* \rho_{23}(0) + \beta_1^* \rho_{23}(1)], \quad (\text{B10})$$

$$D_{21}(1) = i\alpha^*[L_2(1) + L_1(1)]\rho_{21}(1), \quad (\text{B11})$$

$$D_{23}(0) = iL_2(0)\text{Im}[\alpha^* \rho_{21}(0)] + i[L_2(0) + L_3(0)][\beta_0^* \rho_{23}(0) + \beta_1^* \rho_{23}(1)], \quad (\text{B12})$$

$$D_{23}(1) = i\alpha^* L_2(1)\rho_{21}(1), \quad (\text{B13})$$

$$\rho_{21}(0) = i\alpha l_{21}(0)D_{21}(0) - i\beta_0 l_{21}(0)\rho_{31}(0), \quad (\text{B14})$$

$$\rho_{23}(0) = -i\alpha l_{23}(0)\rho_{31}^*(0), \quad (\text{B15})$$

$$\rho_{21}(1) = i\alpha l_{21}(1)D_{21}(1) - i\beta_0 l_{21}(1)\rho_{31}(1) - i\beta_1 l_{21}(1)\rho_{31}(0), \quad (\text{B16})$$

$$\rho_{23}(1) = i\beta_0 l_{23}(1)D_{23}(1) + i\beta_1 l_{23}(1)D_{23}(0) - i\alpha l_{23}(1)\rho_{31}^*(-1), \quad (\text{B17})$$

$$\rho_{31}(0) = i\alpha l_{31}(0)\rho_{23}^*(0) - i\beta_0^* l_{31}(0)\rho_{21}(0) - i\beta_1^* l_{31}(0)\rho_{21}(1), \quad (\text{B18})$$

$$\rho_{31}(1) = -i\beta_0^* l_{31}(1)\rho_{21}(1), \quad (\text{B19})$$

$$\rho_{31}(-1) = -i\beta_1^* l_{31}(-1)\rho_{21}(0). \quad (\text{B20})$$

After some substitutions and elimination of the higher-order terms, the linear system above becomes (when $\Gamma_i = \Gamma$)

$$\rho_{21}(0) = i\alpha l_{21}(0)D_{21}(0) \frac{\{1 + |\beta_1|^2 l_{31}(0)l_{21}(1)[1 + |\beta_0|^2 l_{31}(0)l_{21}(0)]\}}{[1 + |\beta_0|^2 l_{31}(0)l_{21}(0)][1 + |\beta_1|^2 l_{31}(0)l_{21}(1)]}, \quad (\text{B21})$$

$$\rho_{23}(0) = -i|\alpha|^2 \beta_0 l_{23}(0)l_{31}^*(0)l_{21}^*(0)D_{21}(0) \left[\frac{1}{1 + |\beta_1|^2 l_{31}^*(0)l_{21}^*(1)} \right] \quad (\text{B22})$$

$$\rho_{23}(1) = -n_1^0 \left[C + \frac{B}{1 + \frac{4}{\Gamma} \text{Im}(\beta_1^* B)} \left[-\frac{2|\alpha|^2}{\Gamma} \text{Re} \left[\frac{l_{21}(0)}{[1 + |\beta_0|^2 l_{31}(0)l_{21}(0)]} \right] + \frac{2}{\Gamma} \text{Im}[\alpha^* \beta_0 \beta_1^* l_{31}(0)l_{21}(0)E] - \frac{4}{\Gamma} \text{Im}(\beta_0^* A + \beta_1^* C) \right] \right], \quad (\text{B23})$$

where

$$A = -i|\alpha|^2 \beta_0 l_{23}(0)l_{31}^*(0)l_{21}^*(0) \left[\frac{1}{1 + |\beta_1|^2 l_{31}^*(0)l_{21}^*(1)} \right], \quad (\text{B24})$$

$$B = i\beta_1 l_{23}(1), \quad (\text{B25})$$

$$C = -i|\alpha|^2 \beta_1 l_{23}(1) \left[l_{31}^*(-1)l_{21}^*(0) - \frac{|\beta_0|^2 l_{31}(0)l_{21}(1)l_{21}(0)}{(\Gamma - i\delta)[1 + |\beta_1|^2 l_{31}(0)l_{21}(1)]} \right], \quad (\text{B26})$$

$$E = -i\alpha \beta_0^* \beta_1 l_{31}(0)l_{21}(1)l_{21}(0) \left[1 + \frac{|\alpha|^2 l_{31}(0)l_{23}^*(0)}{1 + |\beta_1|^2 l_{31}(0)l_{21}(1)} \right]^{-1} \times \left[1 + |\beta_1|^2 l_{31}(0)l_{21}(1) + |\beta_0|^2 l_{31}(0)l_{21}(0) + |\beta_0|^2 l_{31}(1)l_{21}(1) + \frac{2|\alpha|^2 l_{21}(1)}{\Gamma - i\delta} \right]. \quad (\text{B27})$$

If we now suppose that all the relaxation times are equal $\gamma_{jk} = \Gamma_j = \gamma$, we obtain the simplified results

$$\rho_{21}(0) = -n_1^0 \frac{\alpha}{\Delta} \left[1 + i \frac{\gamma}{\Delta} \left[1 + \frac{|\beta_0|^2}{\gamma} \frac{1}{1 + |\beta_1|^2/\gamma^2} \right] \right], \quad (\text{B28})$$

$$\rho_{23}(0) = in_1^0 \frac{\beta_0}{\gamma} \frac{|\alpha|^2}{\Delta^2} \frac{1}{1 + |\beta_1|^2/\gamma^2}, \quad (\text{B29})$$

$$\rho_{23}(1) = in_1^0 \frac{\beta_1}{\gamma} \frac{|\alpha|^2}{\Delta^2} \frac{1}{1 + |\beta_1|^2/\gamma^2} \frac{1}{1 + 4|\beta_1|^2/\gamma^2} \times \left[1 - 3 \frac{|\beta_0|^2}{\gamma^2} + \frac{|\beta_1|^2}{\gamma^2} \right]. \quad (\text{B30})$$

These expressions are discussed in detail in Ref. 12 together with the different contributions to the matrix elements which are straightforwardly obtained by back substitution.

APPENDIX C

As described in Sec. VB we show here how to obtain information on the asymptotic state from the bichromatic Raman-Raman mode picture. The details of steplike phase locking are also studied.

To define the bichromatic Raman-Raman modes we must return to the original complex evolution equations and recast them in the form

$$\frac{d}{dz} \begin{pmatrix} \mu_0 \\ \beta_0 \end{pmatrix} = \underline{M} \begin{pmatrix} \mu_0 \\ \beta_0 \end{pmatrix}, \quad (\text{C1})$$

where the complex 2×2 matrix \underline{M} is considered to be an implicit function of z via μ_1 and β_1 . The following eigenvalue equation defines the natural bichromatic modes indexed by $+$ and $-$:

$$\underline{M} \begin{pmatrix} \mu_{0\pm} \\ \beta_{0\pm} \end{pmatrix} = \lambda_{\pm} \begin{pmatrix} \mu_{0\pm} \\ \beta_{0\pm} \end{pmatrix}. \quad (\text{C2})$$

A z -dependent linear decomposition of the Raman amplitudes can be performed,

$$\begin{pmatrix} \mu_0 \\ \beta_0 \end{pmatrix} = C_+ \begin{pmatrix} \mu_{0+} \\ \beta_{0+} \end{pmatrix} + C_- \begin{pmatrix} \mu_{0-} \\ \beta_{0-} \end{pmatrix}. \quad (\text{C3})$$

The new evolution equation then reads

$$\frac{d}{dz} \begin{pmatrix} \mu_0 \\ \beta_0 \end{pmatrix} = \lambda_+ C_+ \begin{pmatrix} \mu_{0+} \\ \beta_{0+} \end{pmatrix} + \lambda_- C_- \begin{pmatrix} \mu_{0-} \\ \beta_{0-} \end{pmatrix}. \quad (\text{C4})$$

Despite the fact that we do not succeed in obtaining simple evolution equations for C_{\pm} due to the z dependence of \underline{M} , we can still show that the bichromatic Raman-Raman modes have the following several useful

properties:

- They have no dispersion because λ_{\pm} are both real.
- They are always amplified because $\lambda_+ > \lambda_- > 0$.
- Their global phase is well defined: $\Phi_+ = \pi$, $\Phi_- = 0$.
- Their components obey the specific relationships

$$G_{01} \lesseqgtr G_{23} \Leftrightarrow |\mu_{0+}| \lesseqgtr |\beta_{0+}| \text{ and } |\mu_{0-}| \gtrless |\beta_{0-}|. \quad (\text{C5})$$

The last property allows us to conclude that the dominant Raman component of the more strongly amplified bichromatic mode (with the greatest eigenvalue λ_+) is on the transition where the small signal gain is greater. In the long run, the state of the Raman modes tends to the bichromatic state for which the global phase is π in agreement with the phase locking equation (36).

Finally, the special case ($\Phi=0$), not investigated analytically in the previous letter,¹³ is easy to treat in this picture. Without restriction of generality let us assume that $\mu_0, \mu_1, \beta_0, \beta_1$ are real. To simplify, we will also suppose that μ_1 and β_1 will not change with distance z . The initial conditions ($\mu_0, \mu_1, \beta_0, \beta_1$) at $z=0$ define in a unique manner $C_{\pm}(z=0) = C_{0\pm}$. Let us study the solutions of the equations,

$$\mu_0(z) = 0, \quad \beta_0(z) = 0, \quad (\text{C6})$$

obtained from (C3),

$$z_{\mu} = \left[\frac{1}{\lambda_+ - \lambda_-} \right] \ln \left[- \left[\frac{C_{0-}}{C_{0+}} \right] \right], \quad (\text{C7})$$

$$z_{\beta} = \left[\frac{1}{\lambda_+ - \lambda_-} \right] \ln \left[- \left[\frac{C_{0-}}{C_{0+}} \right] \left[\frac{\beta_{0+}}{\beta_{0-}} \right] \right]. \quad (\text{C8})$$

One can show that always $\beta_{0+}/\beta_{0-} < 0$. Therefore the arguments of the logarithms above have opposite signs and only one of the solutions z_{β} or z_{μ} is defined at a time. This solution will be denoted z_0 . Moreover, it is possible to show by working out the signs of $C_{0\pm}$ as a function of $\mu_0, \mu_1, \beta_0, \beta_1$ ($z=0$) that if $\Phi(z=0) = \pi$, then $z_0 = -\infty$; if $\Phi(z=0) = 0$, then a solution z_0 such that $0 < z < \infty$ always exists and is given by (C6) or (C7). Moreover if $z > z_0$ then $\Phi(z) = \pi$. To summarize, if the initial phase Φ is equal to π the solution is stable, and if the initial phase is equal to zero, an exactly steplike phase locking occurs at z_0 .

If μ_1 and β_1 do not vary too much with distance [or if we are close to the point where $\mu_0(z) = 0$ or $\beta_0(z) = 0$] (C6) or (C7) will permit us to estimate the position at which this phenomenon occurs. This special kind of trajectory in the phase space is continuously approached by varying infinitesimally the initial condition and therefore no "catastrophe" occurs in the structure of the phase space of the system. A numerical example of $\Phi \approx 0$ has been given in Ref. 13.

*Present address: Research Institute for Theoretical Physics, University of Helsinki, Siltavuorenpenger 20 C, SF-00170 Helsinki 17, Finland.

¹R. Behn, I. Kjelberg, P. D. Morgan, T. Okada, and M. R. Siegrist, *J. Appl. Phys.* **54**, 2995 (1983).

²B. G. Danly, S. G. Evangelides, R. J. Temkin, and B. Lax, *IEEE J. Quantum Electron.* **QE-20**, 834 (1984).

³A. Semet, L. C. Johnson, and D. K. Mansfield, *Int. J. Infrared Millimeter Waves* **4**, 231 (1983).

⁴T. A. DeTemple and E. J. Danielewicz, in *Infrared and Milli-*

- meter Waves*, edited by K. J. Button (Academic, New York, 1983), Vol. 7, pp. 1–41.
- ⁵T. A. DeTemple, in *Infrared and Millimeter Waves*, edited by K. J. Button (Academic, New York, 1979), pp. 1–75.
- ⁶B. G. Danly, S. G. Evangelides, R. J. Temkin, and B. Lax, in *Infrared and Millimeter Waves*, edited by K. J. Button (Academic, New York, 1984), pp. 195–278.
- ⁷P. Woskoboinkow, W. J. Mulligan, and R. Erickson, *IEEE J. Quantum Electron.* **QE-19**, 4 (1983).
- ⁸R. G. Harrison, and P. K. Gupta, in *Infrared and Millimeter Waves*, edited by K. J. Button (Academic, New York, 1983), pp. 43–118.
- ⁹F. Julien, J. M. Lourtioz, T. A. DeTemple, and S. J. Petuchowski, *Opt. Commun.* **54**, 246 (1985).
- ¹⁰B. Wellegehausen, *IEEE J. Quantum Electron.* **QE-15**, 1108 (1979).
- ¹¹M. S. Malcuit, D. J. Gauthier, and R. W. Boyd, *Phys. Rev. Lett.* **55**, 1086 (1985).
- ¹²M. A. Dupertuis, R. R. E. Salomaa, and M. R. Siegrist, *Phys. Rev. A* **30**, 2824 (1984).
- ¹³M. A. Dupertuis, R. R. E. Salomaa, and M. R. Siegrist, *Opt. Commun.* **54**, 27 (1985).
- ¹⁴L. A. Lugiato, *Z. Phys. B* **41**, 85 (1981).
- ¹⁵G. Dodel and N. G. Douglas, *IEEE J. Quantum Electron.* **QE-18**, 1294 (1982).
- ¹⁶M. Sargent III, M. O. Scully, and W. E. Lamb, *Laser Physics* (Addison Wesley, Reading, Mass., 1974).
- ¹⁷M. A. Dupertuis, R. R. E. Salomaa, and M. R. Siegrist, *IEEE J. Quantum Electron.* **QE-20**, 440 (1984).
- ¹⁸M. A. Dupertuis, R. R. E. Salomaa, and M. R. Siegrist, *IEEE J. Quantum Electron.* (to be published).
- ¹⁹R. R. E. Salomaa, *J. Phys. B* **11**, 3745 (1978).
- ²⁰M. A. Dupertuis, R. R. E. Salomaa, and M. R. Siegrist, *Opt. Commun.* **57**, 410 (1986).
- ²¹B. D. Fried and S. D. Conte, *The plasma dispersion function* (Academic, New York, 1961).
- ²²S. J. Petuchowski, J. D. Oberstar, T. A. DeTemple, *Phys. Rev. A* **20**, 529 (1979).
- ²³Note that a factor of 2 is missing in Eq. (9) of Ref. 13.
- ²⁴S. T. Hendow and M. Sargent III, *Opt. Commun.* **40**, 385 (1982).
- ²⁵S. T. Hendow and M. Sargent III, *Opt. Commun.* **43**, 59 (1982).
- ²⁶L. W. Hillman, R. W. Boyd, and C. W. Stroud, *Opt. Lett.* **7**, 426 (1982).
- ²⁷J. P. Nicholson, *Opt. Commun.* **29**, 49 (1979).
- ²⁸P. Woskoboinkow, H. C. Praddaude, W. J. Mulligan, D. R. Cohn, and B. Lax, *J. Appl. Phys.* **50**, 1125 (1979).
- ²⁹S. J. Petuchowski and T. A. DeTemple, *Int. J. Infrared Millimeter Waves* **1**, 387 (1980).
- ³⁰J. D. Wiggins, Z. Drozdowicz, and R. J. Temkin, *IEEE J. Quantum Electron.* **QE-14**, 23 (1978).
- ³¹A. De Martino, R. Frey, and F. Pradère, *Opt. Commun.* **27**, 262 (1978).
- ³²P. Woskoboinkow, J. S. Machuzak, and W. J. Mulligan, *IEEE J. Quantum Electron.* **QE-21**, 14 (1985).
- ³³Pump resonance $R(3)$ leads to signal emission on $Q(3)$, $v=1$ and on $Q(4)$, $v=0$ (see Fig. 8).
- ³⁴H. K. Chung, J. B. Lee, and T. A. DeTemple, *Opt. Commun.* **39**, 105 (1981).
- ³⁵F. A. Hopf, P. Meystre, M. O. Scully, and J. F. Seely, *Phys. Lett.* **35**, 511 (1975).
- ³⁶Lin Yikun, Qiu Bingshen, Gong Di, and Guo Bingyin, *Int. J. Infrared Millimeter Waves* **3**, 553 (1982).
- ³⁷R. Behn, M. A. Dupertuis, I. Kjelberg, P. A. Krug, S. A. Salito, and M. R. Siegrist, *Time-resolved Linewidth and Lineshape Measurements of an Optically-Pumped Far Infrared D₂O Laser*, Proceedings of the 11th International Conference on Infrared and Millimeter Waves, Tirrenia, Pisa, Italy, 1986, pp. 377–379 [*IEEE J. Quant. Electron.* (to be published)].
- ³⁸J. R. Izatt, B. K. Deka, and W. Zhu, *IEEE J. Quantum Electron.* **QE-23**, 117 (1987).